Original Article

Adipose tissue macrophage-derived exosomal miR-210-5p in modulating insulin sensitivity in rats born small for gestational age with catch-up growth

Hui Xiong[1#], Wei Liu[1#], Jie Song[2#], Xia Gu[1], Shunchang Luo[1], Zhendong Lu[1], Hu Hao[1], Xin Xiao[1]

[1]Department of Pediatrics, The Sixth Affiliated Hospital, Sun Yat-sen University, Guangzhou, China; [2]Department of Pediatrics, The Fifth Affiliated Hospital, Sun Yat-sen University, Zhuhai, China

Contributions: (I) Conception and design: X Xiao, H Xiong, W Liu; (II) Administrative support: X Xiao; (III) Provision of study materials or patients: H Xiong, S Luo, Z Lu; (IV) Collection and assembly of data: J Song, X Gu; (V) Data analysis and interpretation: J Song, H Hao; (VI) Manuscript writing: All authors; (VII) Final approval of manuscript: All authors.

[#]These authors contributed equally to this work as co-first authors.

Correspondence to: Xin Xiao, MD. Department of Pediatrics, The Sixth Affiliated Hospital, Sun Yat-sen University, No. 26, Erheng Road, Yuancun, Tianhe District, Guangzhou 510655, China. Email: xiaoxin2@mail.sysu.edu.cn.

Background: Insulin resistance has been implicated in the pathogenesis of children born small for gestational age (SGA) with catch-up growth (CUG). Adipose tissue macrophages (ATMs) regulate insulin resistance by secreting exosomes containing microRNA (miRNA) cargo; however, their pathogenic roles and molecular mechanism are not fully understood. This study aimed to investigate the role of miR-210-5p in rats born SGA with CUG and insulin resistance.

Methods: The dietary needs of pregnant rats were restricted to ensure the birth of SGA rats. Transmission electron microscopy (TEM) and Western blot analysis were used to identify the exosomes from ATMs of CUG-SGA and adequate-for-gestational-age (AGA) rats. PKH-67 staining was performed to confirm the uptake of exosomes. miR-210-5p expression was measured by quantitative reverse transcription polymerase chain reaction (qRT-PCR). Glucose uptake and output were detected with glucose uptake and output assays, respectively. Insulin resistance was detected with glucose and insulin tolerance tests *in vivo*. The interaction between miR-210-5p and SID1 transmembrane family member 2 (SIDT2) was validated with dual-luciferase reporter assay.

Results: miR-210-5p was observed to be highly expressed in the exosomes derived from the ATMs of CUG-SGA rats. ATM-derived exosomes can serve as vehicles to deliver miR-210-5p into adipocytes, myocytes, and hepatocytes, where it can enhance cellular insulin resistance. *SIDT2* was identified as a direct target gene of miR-210-5p. The miR-210-5p–induced insulin resistance was reversed by the restored SIDT2 expression. However, overexpression of SIDT2 abolished the inhibitory effect of CUG-SGA-ATM-exosomal miR-210-5p on insulin sensitivity *in vivo*.

Conclusions: ATM-derived exosomal miR-210-5p promoted insulin resistance in CUG-SGA rats by targeting *SIDT2*, which may act as a new potential therapeutic target for children born SGA with CUG.

Keywords: Insulin resistance; macrophages; miR-210-5p; small-for-gestational-age; catch-up growth (CUG)

Submitted Dec 28, 2022. Accepted for publication Apr 17, 2023. Published online Apr 26, 2023.
doi: 10.21037/tp-23-142
View this article at: https://dx.doi.org/10.21037/tp-23-142

Introduction

The incidence of children born small for gestational age (SGA) is a common medical concern occurring in 8–26% of all infants born worldwide (1). It is defined as having a birth weight and/or length standard deviation score (SDS) of <–2 (2,3). Approximately 85–90% of children born SGA complete postnatal catch-up growth (CUG) within the first 2 years and maintain a height comparable to their peers (2). CUG is commonly defined as height-for-age z score (HAZ) of >–2 SD (4,5). Macrophages are the most important inflammatory cells in adipose tissue of obese, and play a key role in insulin resistance (6,7). Children born SGA with CUG have been reported to have fat accumulation, abnormal adipocyte function, and development of adipose tissue caused by adverse intrauterine growth (8,9). Excess fat accumulation can lead to free fatty acid (FFA) release, and high concentrations of FFA can induce insulin resistance in the muscle and liver (10,11). Thus, to develop strategies to prevent insulin resistance, it is crucial to understand the relative contribution of CUG to the emergence of the condition.

Exosomes are vesicles that range in size from 40 to 100 nm and are released from various types of tissues and cells. They are involved in several biological processes and the pathogenesis of human disorders, such as the development of cancer and various metabolic diseases (12).

Highlight box

Key findings

- Adipose tissue macrophage-derived exosomal microRNA (miR)-210-5p modulates insulin sensitivity in rats born small for gestational age with catch-up growth by targeting SID1 transmembrane family member 2 (SIDT2).

What is known and what is new?

- miR-210-5p is markedly upregulated in the exosomes derived from adipose tissue macrophages (ATMs). miR-210-5p in exosomes derived from high glucose-induced macrophage RAW264.7 cells inhibited glucose uptake and mitochondrial complex IV (CIV) complex activity in 3T3-L1 adipocytes.
- In rats born small for gestational age with catch-up growth, insulin sensitivity was found to be modulated by exosomal miR-210-5p, which was derived from adipose tissue macrophages and targeted SIDT2..

What is the implication, and what should change now?

- The results of this study can clarify the role of miR-210-5p in rats born small for gestational with catch-up growth and insulin resistance.

Exosomes transport cargo such as proteins, RNA and lipids that can be used to transmit information within cells (13). MicroRNAs (miRNAs) are a class of highly conserved, endogenous, single-stranded noncoding small RNAs that regulate gene expression by binding to the 3' untranslated region (UTR) of target mRNA, causing translational arrest or degradation (14). Emerging evidence has revealed that exosomal miRNAs play a crucial role in insulin resistance and glucose intolerance in both animals and humans (15,16). For example, adipose tissue macrophage (ATM)–derived exosomal miR-155 can cause insulin resistance *in vivo* and *in vitro* (17). Moreover, exosomal transfer of obesity adipose tissue for decreased miR-141-3p inhibited the insulin sensitivity and glucose uptake of hepatocytes (18). Currently, miR-210-5p has been reported to be markedly upregulated in the exosomes derived from ATM (17), and exosomal miRNA-210 disrupts adipocyte glucose mitochondrial oxidation and glucose uptake (12). Moreover, miR-210-5p is correlated with fasting glucose levels and fasting insulin (19). However, the expression and molecular mechanisms of miR-210-5p in rats born SGA with CUG (CUG-SGA) remain poorly understood.

This study aimed to investigate how functional gene expression regulation affects the influence of miR-210-5p on CUG-SGA rats. The findings of this investigation may provide novel insights into how miRNAs mediate the pathogenesis of children born CUG with SGA. We present the following article in accordance with the ARRIVE reporting checklist (available at https://tp.amegroups.com/article/view/10.21037/tp-23-142/rc).

Methods

Establishment of the Animal Model

A protocol was prepared before the study without registration. All animal procedures complied with institutional guidelines for the care and use of animals, and the protocols were approved by the Institutional Animal Ethics Committee of The Sixth Affiliated Hospital, Sun Yat-sen University (No. IACUC-2021092702). A total of 10 specific pathogen-free (SPF)–grade healthy females and 5 SPF-grade healthy eight-week-old male Sprague-Dawley rats (weight 230–320 g) were obtained from the Animal Center of Charles River (Zhejiang, China) and fed at The Sixth Affiliated Hospital, Sun Yat-sen University in China. Pregnant rats subjected to dietary restriction were used to establish a rat model of SGA. Female and

male rats (2:1) were caged randomly. Daily vaginal smears were examined under a standard optical microscope, and the day sperm first appeared in the smear was considered to be day 1 of pregnancy. A total of 10 pregnant rats were randomly divided into 2 groups (n=5 per group): control and SGA groups. Pregnant rats in the control group were fed a standard food diet available ad libitum throughout pregnancy, whereas pregnant rats in the SGA group were subjected to food restriction (50% of normal intake) starting the day after conception. All pregnant rats gave birth naturally. All pups were breastfed for the first 3 weeks after birth and then fed with standard chow. The weight and nose-to-anus length of all the pups were measured at birth, and the litter sizes were recorded. The size of the litter was adjusted to 5 pups per litter to ensure the CUG of the offspring with SGA. SGA infant rats were defined as those with neonatal body weight or body length that was less than 2 SD below the average values in the control group. Body weight and length were measured weekly. CUG-SGA rats were identified when the body weight and body length were –2 SD higher than those in the control group at 4 weeks of age (11,20,21).

Glucose tolerance test and insulin tolerance test

Following a 16-h overnight fast, rats underwent the glucose tolerance test. Each rat was intragastrically administered with glucose (2 g/kg), and the blood glucose levels were measured in each rat at 0, 30, 60, 90 and 120 min post-administration using a blood glucose meter. The insulin tolerance test was performed following a 6-h fast. Each rat was intraperitoneally administered insulin (0.70 units/kg), and the blood glucose levels were evaluated at 0, 15, 30, 45, and 60 min post-injection.

Glucose uptake assay

Glucose levels of extracted cells were assessed using the Glucose Uptake-Glo Assay (Promega, Madison, WI, USA). Following 8 h of serum starvation, 3T3-L1 adipocytes and L6 myocytes were incubated with 100 nM of insulin for 30 min at 37 ℃. Cells were washed twice with phosphate buffered solution (PBS), and 1 mM of 2-deoxyglucose (2DG) was added and incubated for 15 min at 37 ℃. Subsequently, Stop Solution (lysis buffer) and neutralization buffer were added, and the mixture was incubated for 10 min at 37 ℃. The labelled 2DG-6-phosphate solution was then added. A luminometer (Luminoskan Ascent, Thermo Fisher Scientific) was used to measure the luminescence (22).

Primary hepatocyte isolation

The liver isolated from 4-week-old adequate-for-gestational-age (AGA) rats was perfused with Hanks' balanced salt solution (Gibco) and then digested with collagenase type IV solution (Gibco). The dissociated cells were filtered through a 100 mm nylon filter and centrifuged at 35 g for 5 min at 4 ℃. Cells were washed twice with PBS and centrifuged at 500 rpm for 5 min at 4 ℃. Finally, cells were resuspended and seeded onto a 6-well plate in Dulbecco's modification of Eagle's medium Dulbecco (DMEM) containing 10% FBS.

ATMs isolation

ATMs were isolated from adipose tissues of CUG-SGA (CUG-SGA-ATMs) or AGA rats (AGA-ATMs) using a rat F4/80$^+$ macrophage isolation kit (Miltenyi Biotec GmbH, Bergisch-Gladbach, Germany) according to the manufacturer's instructions. Single-cell suspensions were incubated with fluorescence-tagged antibodies against F4/80. The stained cells were run on a BD FACSAria cell sorter (BD Biosciences, Franklin Lakes, NY, USA). Data were analyzed using the CellQuest software program (BD Biosciences). ATMs were cultured in Iscove's Modified Dulbecco's Media (IMDM) containing 10% exosome-free FBS to produce exosomes.

Exosome isolation, identification, labeling, and incubation assay

Exosomes were extracted from the supernatant of adipose tissue macrophages (ATMs) with ExoQuick-TCTM (System Biosciences, Palo Alto, CA, USA) following the manufacturer's protocol. The final exosomes were resuspended in phosphate-buffered saline (PBS) and stored at –80 ℃ for long-term preservation. The collected exosomes were identified using transmission electron microscopy (TEM) and Western blotting for CD9 and CD63, as previously described. The concentration of exosomes was determined by using a bicinchoninic acid (BCA) protein assay kit (Thermo Fisher Scientific, Waltham, MA, USA) according to the manufacturer's instructions. Following the manufacturer's instructions, purified exosomes were labeled with the membrane-labelling dye PKH67 Green Fluorescent Linker Mini Kit

(Sigma-Aldrich, St. Louis, MO, USA). Two micrograms of exosomes were incubated with 1×10^5 3T3-L1 adipocytes, L6 myocytes, and primary hepatocytes. After 6 h, cells were harvested for miR-210-5p expression assays.

Cell culture

The mouse 3T3-L1 adipocytes and rat L6 myocytes were obtained from Jennio Biotech (Guangzhou, China). All cells were cultured in Dulbecco's Modified Eagle's Medium (DMEM; Gibco, Carlsbad, CA, USA) containing 1% penicillin-streptomycin (Gibco, Thermo Fisher Scientific) and 10% fetal bovine serum (FBS; Gibco) in a 37 ℃ incubator (5% CO_2).

Cell transfection

The miR-210-5p and control mimics were synthesized by RiboBio (Guangzhou, China). For overexpression of SID1 transmembrane family member 2 (SIDT2), the coding sequences were amplified by polymerase chain reaction (PCR) and ligated with pcDNA3.0 plasmid. Through use of the Lipofectamine 2000 reagent (Thermo Fisher Scientific, USA), the miR-210-5p mimics, control mimics, and SIDT2 plasmid were transfected into 3T3-L1 adipocytes, L6 myocytes, and primary hepatocytes as per the manufacturer's instructions.

Glucose output assay

After the rats underwent 12-serum fasting, primary hepatocytes were washed with PBS twice and subjected to glucose-free buffer supplemented with glucagon (100 ng/mL), insulin (10 nM) or a combination of glucagon and insulin for 30 min at 37 ℃. A glucose assay kit (Applygen Technologies Inc., Beijing, China) was used to measure the glucose concentration. A twofold concentration of the kit reagents was applied to enhance the sensitivity. The cells were collected and lysed using a radioimmunoprecipitation assay buffer. The total protein concentration was detected using a BCA protein assay kit (Beyotime Biotechnology, Jiangsu, China) to normalize the glucose output (23).

Dual-luciferase reporter assay

A luciferase construct containing 3'-UTR of SIDT2 with the wild-type (SIDT2-wt) or a mutated version of the binding site (SIDT2-mut) was cotransfected with miR-210-5p or control mimics into 3T3-L1 adipocytes, L6 myocytes, and primary hepatocytes. Cells were collected 48 h after cell transfection, and dual-luciferase activity was measured following the manufacturer's instructions using a dual-luciferase reporter assay (RiboBio).

In vivo exosome treatment

A total of 25 healthy four-week-old AGA rats were randomly divided into 5 groups (n=5 per group): normal AGA rats treated with 0.2 mL of PBS, AGA rats treated with AGA-ATM–derived exosomes (AGA-ATM-exos, 30 μg every 7 days) via the tail vein, AGA rats treated with CUG-SGA-ATM-exos (30 μg every 7 days) via the tail vein, AGA rats with treated with CUG-SGA-ATM-exos (30 μg every 7 days) + negative control (NC) plasmid (30 μg every 7 days) via the tail vein, and AGA rats treated with CUG-SGA-ATM-exos (30 μg every 7 days) + SIDT2 plasmid (30 μg every 7 days) via the tail vein. After 4 weeks, rats were fasted for the measurement of blood glucose levels, serum insulin, and glucose and insulin tolerance tests. The formula used to calculate the index of homeostasis model assessment of the insulin resistance (HOMA-IR) was as follows: fasting blood glucose level (mmol/L)/fasting serum insulin level (mU/mL)/22.5.

Western blotting

Sodium dodecyl-sulphate polyacrylamide gel electrophoresis gel was used to isolate 20 μg of total protein, which was then transferred onto polyvinylidene fluoride membranes (MilliporeSigma, Burlington, MA, USA) and enclosed with 5% skim milk. The membranes were incubated overnight with the primary antibody targeting phosphorylated-AKT (p-AKT) (1:1,000; Abcam, Cambridge, UK), AKT (1:10,000; Abcam), SIDT2 (1:1,000, Abbexa, Cambridge, UK), or GAPDH (1:5000; Abcam) at 4 ℃, which was followed by incubation with horseradish peroxidase–linked secondary antibodies at room temperature for 1 h. The protein band was visualized using a chemiluminescence substrate (Pierce Chemical, Rockford, IL, USA).

qRT-PCR

Total RNA in cells, tissues, was exosomes were extracted using TRIzol reagent (Invitrogen) following the manufacturer's instructions. miRNA and messenger RNA (mRNA) reverse transcriptions were conducted with a

miRNA complement DNA (cDNA) synthesis kit (Applied Biological Materials, Zhenjiang, China) and M-MLV (Moloney Murine Leukemia Virus) reverse transcriptase (Invitrogen), respectively. Quantitative reverse transcription polymerase chain reaction (qRT-PCR) was measured using the SYBR green PCR master mix (Takara Bio, Kusatsu, Japan) on an ABI 7900 fast real-time PCR system (Applied Biosystems, Thermo Fisher Scientific). SIDT2 and miR-210-5p expression levels were normalized to the internal controls (U6 and β-actin), and the relative expression levels were evaluated using the $2^{-\Delta\Delta CT}$ method. The sequences of all indicated primers used are presented in Table S1.

Statistical analyses

Data are presented as mean ± SD. Statistical analyses were performed using SPSS 17.0 (IBM Corp., Armonk, NY, USA) and GraphPad Prism 8.0. (GraphPad Software, San Diego, CA, USA). Student *t*-test (2-tailed) was used to compare differences between 2 groups, whereas 1-way analysis of variance (ANOVA) or 2-factor ANOVA was used to compare differences between 3 or more groups. $P<0.05$ was regarded as statistically significant.

Results

miR-210-5p levels were elevated in adipose tissues from CUG-SGA rats with insulin resistance

To study changes in insulin resistance, we developed a CUG-SGA rat model. Compared to the AGA group, the CUG-SGA group had higher fasting blood glucose levels, fasting serum insulin, and HOMA-IR index score (*Figure 1A-1C*). In addition, the CUG-SGA group showed increased glucose and insulin tolerance and decreased AKT phosphorylation (*Figure 1D-1F*). The expression of miR-210-5p was significantly higher in the adipose tissues in the CUG-SGA group than in those in the AGA group (*Figure 1G*). Therefore, miR-210-5p may be involved in the development of insulin resistance in CUG-SGA.

ATMs secreted exosomal miR-210-5p

ATMs were isolated from the visceral adipose tissue of CUG-SGA and AGA rats, and their ability to secrete extracellular miR-210-5p was evaluated by flow cytometry. As presented in *Figure 2A*, these cells positively expressed $F4/80^{+}$. Following exosome isolation from the supernatant of ATMs, TEM analysis revealed that they exhibited the characteristic round or cup-shaped morphology and had a diameter of 30–100 nm (*Figure 2B*). The identity of isolated exosomes was further confirmed by the presence of known exosome markers, including proteins CD63 and CD9 (*Figure 2C*). In addition, miR-210-5p was upregulated in the ATMs and ATM-derived exosomes (ATM-exos) of the rats in the CUG-SGA group compared to those in the AGA (*Figure 2D,2E*). Next, we investigated whether ATM-exos could be taken up by 3T3-L1 adipocytes, L6 myocytes, and primary hepatocytes. After PKH67 dye (green) staining, CUG-SGA-ATM-exos or AGA-ATM-exos were cocultured with the recipient cells for 12 h. These cells exhibited efficient ATM-exo uptake upon coculturing as indicated by the presence of green fluorescence staining in the recipient cells (*Figure 2F*). Interestingly, the enhanced expression of miR-210-5p in the recipient cells cocultured with CUG-SGA-ATM-exos was observed (*Figure 2G*). Taken together, our findings demonstrated that macrophages can secrete miR-210-5p–containing exosomes, which are then efficiently transported into these recipient cells.

miR-210-5p reduced cellular insulin sensitivity

To investigate the effects of miR-210-5p on cellular insulin sensitivity, 3T3-L1 adipocytes, L6 myocytes, and primary hepatocytes were transiently transfected with miR-210-5p or control mimics. The transfection efficiency obtained from qRT-PCR is presented in *Figure 3A*. The results from the glucose cellular uptake assay revealed that the overexpression of miR-210-5p resulted in a marked decrease in insulin-stimulated glucose uptake in 3T3-L1 adipocytes and L6 myocytes and exhibited a significant increase in insulin-stimulated glucose output in primary hepatocytes (*Figure 3B-3D*). Consistent with these results, the upregulation of miR-210-5p, which regulates cellular insulin signaling, significantly reduced insulin-stimulated phosphorylation of AKT (*Figure 3E*). Overall, these results suggest that miR-210-5p modulates insulin sensitivity.

SIDT2 was identified as a target of miR-210-5p

The putative target of miR-210-5p implicated in insulin sensitivity was then identified using the computational miRNA target prediction database TargetScan. We observed that the miR-210-5p sequence complemented the 3'-UTR of SIDT2 (*Figure 4A*), and enforced expression

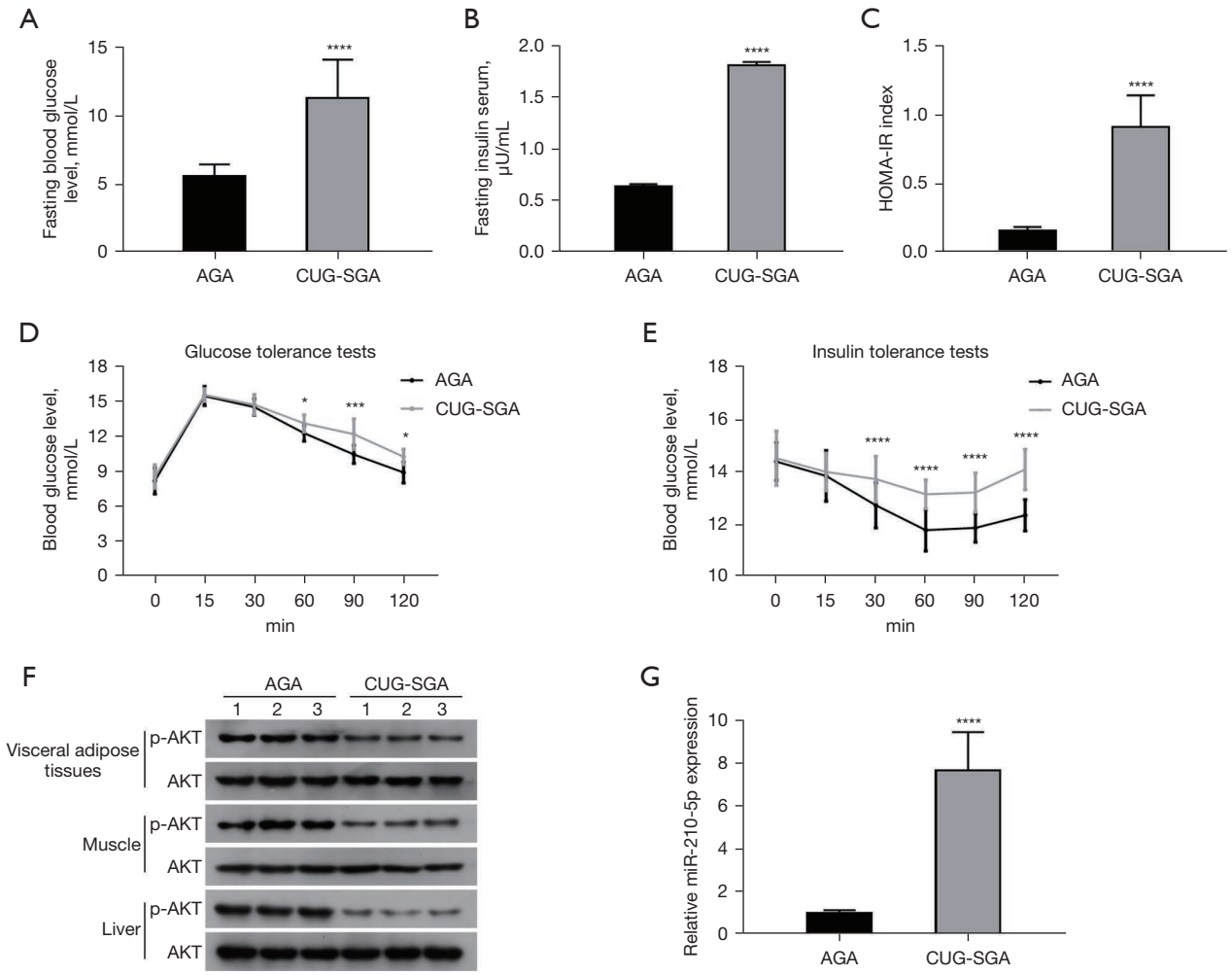

Figure 1 miR-210-5p levels were elevated in the adipose tissues from CUG-SGA rats with insulin resistance. (A-E) Comparison of fasting blood glucose levels, fasting serum insulin, index of HOMA-IR, glucose tolerance, and insulin tolerance of CUG-SGA (n=20) and AGA rats (n=25) rats. (F) Phosphorylation of AKT was detected by Western blotting (n=3). (G) The expression of miR-210-5p in the adipose tissues of CUG-SGA (n=20) and AGA rats (n=25) groups. *, P<0.05, ***, P<0.001, ****, P<0.0001 *vs.* AGA group. CUG-SGA, small-for-gestational-age with catch-up-growth; HOMA-IR, homeostasis model assessment of the insulin resistance; AGA, adequate-for-gestational-age; AKT, protein kinase B.

of miR-210-5p led to reduced mRNA and protein levels of SIDT2 (*Figure 4B-4E*). To further verify the interaction between miR-210-5p and SIDT2, the 3'-UTR of SIDT2 containing the predicted binding site (SIDT2-wt) and its mutation site (SIDT2-mut) were cloned into a luciferase reporter vector. As presented in *Figure 4F-4H*, miR-210-5p enhancement significantly impaired the luciferase intensity of the luciferase reporter vector with SIDT2-wt in 3T3-L1 adipocytes, L6 myocytes, and primary hepatocytes, whereas there was no visible difference in the SIDT2-mut luciferase reporters. Together, these results indicated that *SIDT2* served as a target for miR-210-5p.

SIDT2 partly reversed miR-210-5p–mediated effects on cellular insulin sensitivity

Given that *SIDT2* functions as a target for miR-210-5p, we further investigated whether miR-210-5p exerted its role through SIDT2. As exhibited in *Figure 5A,5B*, decreased mRNA and protein expression of SIDT2 in 3T3-L1 adipocytes, L6 myocytes, and primary hepatocytes induced by miR-210-5p elevation was reversed via

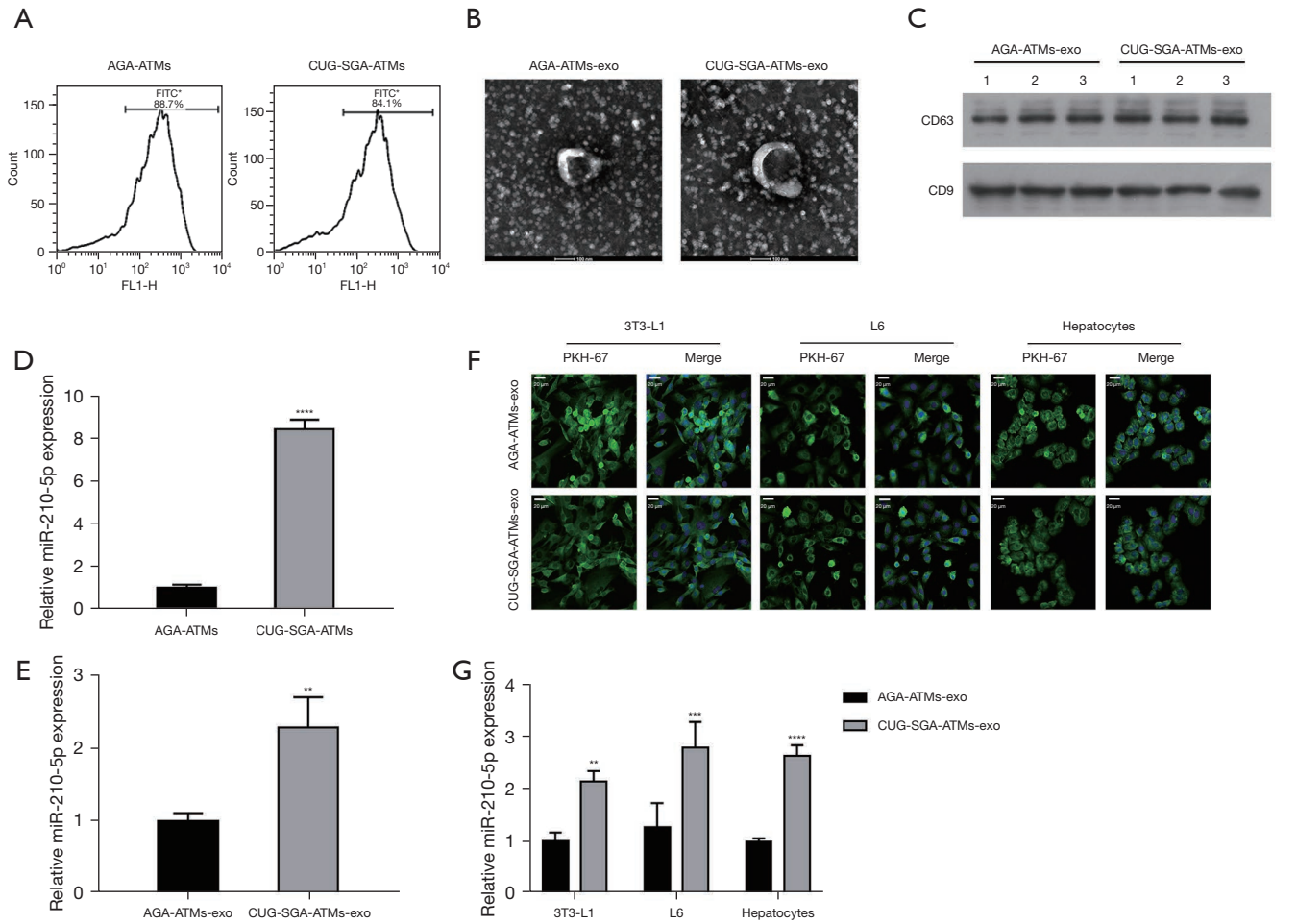

Figure 2 ATMs secreted exosomal miR-210-5p. (A) Flow cytometry of surface markers on ATMs from adipose tissue of CUG-SGA and AGA rats. (B) Transmission electron microscopy images of ATMs-derived exosomes (ATMs-exo) from the adipose tissue of CUG-SGA and AGA rats. (C) Western blot analysis of the exosome marker of CD63 and CD9. (D,E) The levels of miR-210-5p in ATMs and ATMs-exo from the adipose tissue of CUG-SGA and AGA rats were measured using qRT-PCR. (F) Fluorescence images of 3T3-L1 adipocytes, L6 myocytes, and primary hepatocytes incubated with PKH67-labeled CUG-SGA-ATMs-exo or AGA-ATMs-exo (green). (G) qRT-PCR analysis of miR-210-5p expression in the recipient cells cocultured with CUG-SGA-ATMs-exo or AGA-ATMs-exo. Data are expressed as mean ± SD; n=3. **, P<0.01, ***, P<0.001, ****, P<0.0001 *vs.* AGA-ATMs or AGA-ATMs-exo group. ATMs, adipose tissue macrophages; CUG-SGA, small-for-gestational-age with catch-up-growth; AGA, adequate-for-gestational-age; qRT-PCR, quantitative reverse transcription polymerase chain reaction.

SIDT2 overexpression. Moreover, the downregulation of p-AKT in 3T3-L1 adipocytes, L6 myocytes, and primary hepatocytes expressing miR-210-5p was reversed by SIDT2 overexpression (*Figure 5C*). Furthermore, the inhibitory impact of miR-210-5p overexpression on insulin-induced glucose uptake in 3T3-L1 adipocytes and L6 myocytes was abolished by SIDT2 upregulation (*Figure 5D,5E*). In addition, increased SIDT2 expression regained the stimulatory effect on insulin-stimulated glucose production mediated by miR-210-5p mimics in primary hepatocytes (*Figure 5F*). Collectively, these findings indicate that miR-210-5p causes insulin resistance through *SIDT2*.

CUG-SGA ATM–derived exosomal miR-210-5p enhanced in vivo insulin resistance via SIDT2

To further confirm if CUG-SGA-ATM-exos miR-210-5p enhances the insulin resistance via *SIDT2*, CUG-

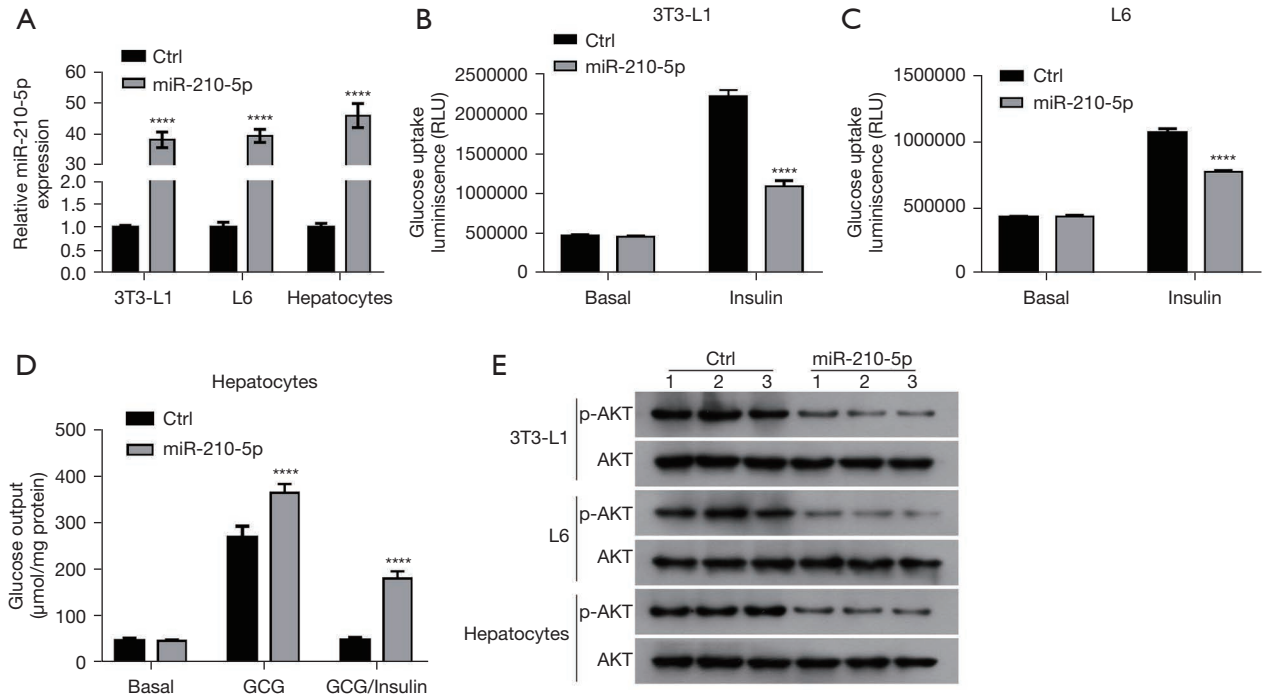

Figure 3 miR-210-5p reduced cellular insulin sensitivity. (A) qRT-PCR analysis verified the overexpression efficiency of miR-210-5p in 3T3-L1 adipocytes, L6 myocytes, and primary hepatocytes. (B-D) The glucose uptake content of 3T3-L1 adipocytes and L6 myocytes and the glucose output content of primary hepatocytes were measured. (E) Western blot assays of p-AKT and AKT expression. Data are expressed as mean ± SD, n=3. ****, P<0.0001 *vs.* control group. GCG, glucagon; qRT-PCR, quantitative reverse transcription polymerase chain reaction; p-AKT, phosphorylated-protein kinase B; AKT, protein kinase B.

SGA-ATM-exos, AGA-ATM-exos, or CUG-SGA-ATM-exos and SIDT2 plasmid were administrated intravenously to insulin-sensitive AGA rats. As predicted from our *in vitro* results, administration of CUG-SGA-ATM-exos promoted insulin resistance as evidenced by elevated fasting blood glucose levels, fasting serum insulin, and HOMA-IR index scores in insulin-sensitive AGA rats; however, SIDT2 augmentation reversed this increased effect (*Figure 6A-6C*). Consistently, SIDT2 overexpression reversed the increase in glucose intolerance and insulin resistance mediated by CUG-SGA-ATM-exos (*Figure 6D,6E*). Furthermore, enhanced SIDT2 expression attenuated the suppressive effect of CUG-SGA-ATM-exos on the phosphorylation of AKT in the liver, adipose, and muscle tissues (*Figure 6F*). Overall, these results indicated that *SIDT2* is a target of CUG-SGA-ATM-exos miR-210-5p that could reduce insulin sensitivity *in vivo*.

Discussion

Emerging evidence suggests that insulin resistance is linked with children born SGA with CUG; however, the molecular mechanisms of insulin resistance in this population remain to be investigated. In this study, we demonstrated that miR-210-5p, which is highly expressed in the ATM-exos derived from the adipose tissue of CUG-SGA rats, can cause insulin resistance *in vitro*. A study of the mechanism revealed that *SIDT2* was a direct target of miR-210-5p. The overexpression of SIDT2 blocked the inhibitory effect of miR-210-5p on insulin sensitivity. Furthermore, the administration of SIDT2 improved insulin resistance induced by CUG-SGA-ATM-exos miR-210-5p treatment.

A growing body of evidence suggests that exosomes containing large amounts of miRNAs function as vehicles for transferring miRNAs to neighboring or distant cells (24). In addition, our study demonstrated that miR-210-5p was upregulated in ATM-exos derived from the adipose tissue of CUG-SGA rats and was further transferred into 3T3-L1 adipocytes, L6 myocytes, and primary hepatocytes. Exosomes from macrophages have been reported to be closely associated with various pathogenic conditions, including insulin sensitivity and

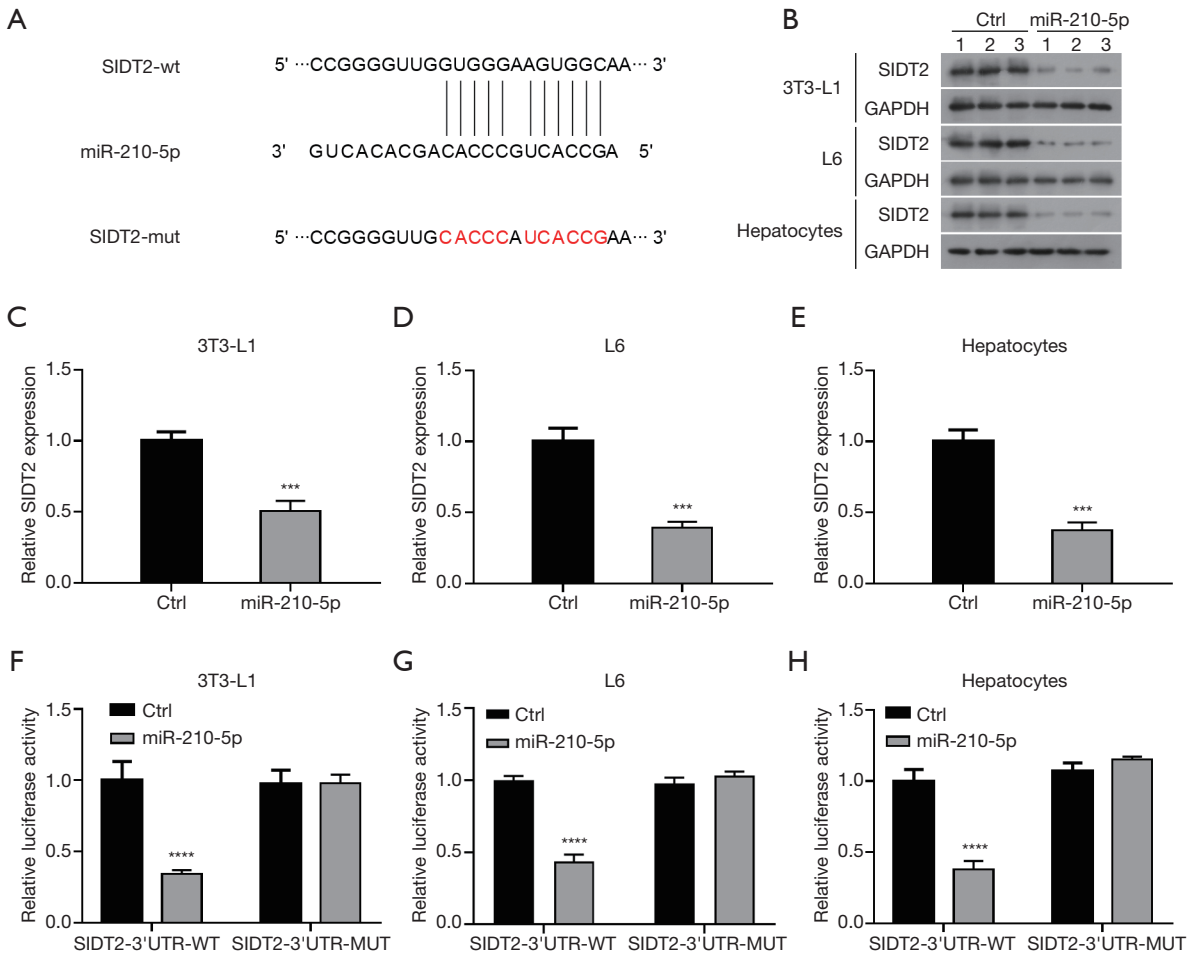

Figure 4 SIDT2 was identified as a target of miR-210-5p. (A) The binding site of miR-210-5p in the 3'-UTR of SIDT2 and its mutant was displayed. (B-E) The mRNA and protein levels of SIDT2 in 3T3-L1 adipocytes, L6 myocytes, and primary hepatocytes transfected with miR-210-5p or control mimics were detected by Western blotting. (F-H) The relative luciferase activity in 3T3-L1 adipocytes, L6 myocytes, and primary hepatocytes cotransfected with a luciferase reporter plasmid containing wild-type SIDT2-wt or SIDT2-mut as well as miR-210-5p or control mimics was analyzed. Data are expressed as mean ± SD, n=3. ***, P<0.001, ****, P<0.0001 *vs.* control group. SIDT2, SID1 transmembrane family member 2; 3'-UTR, 3' untranslated region; SIDT2-wt, wild-type SIDT2; SIDT2-mut, mutated SIDT2; qRT-PCR, quantitative reverse transcription polymerase chain reaction.

cardiac disorders (12,17,25,26). For example, miR-690 within ATM-derived exosomes directly promotes insulin sensitivity both *in vitro* and *in vivo* (26). In obese mice, ATMs secrete miR-155–containing exosomes, which impairs cellular insulin action, *in vivo* insulin sensitivity, and overall glucose homeostasis (17). Moreover, miR-210-5p in exosomes derived from high glucose–induced macrophage RAW264.7 cells have been shown to inhibit glucose uptake and mitochondrial CIV complex activity in 3T3-L1 adipocytes (12). Consistent with this, our findings suggest that CUG-SGA-ATM-exos miR-210-5p repressed glucose uptake and insulin sensitivity *in vitro* while enhancing glucose intolerance and insulin resistance *in vivo*.

miRNAs exert their biological effects by binding to specific sequences in the 3'-UTR of target mRNAs, causing translational arrest or mRNA degradation (15). We identified *SIDT2* as a potential target of miR-210-5p using a bioinformatics approach. SIDT2 is a lysosomal integral membrane protein that is widely expressed in mammalian tissue (27,28). Previous studies have revealed that SIDT2 mediated an array of cellular biological responses, including autophagy, lipid metabolism,

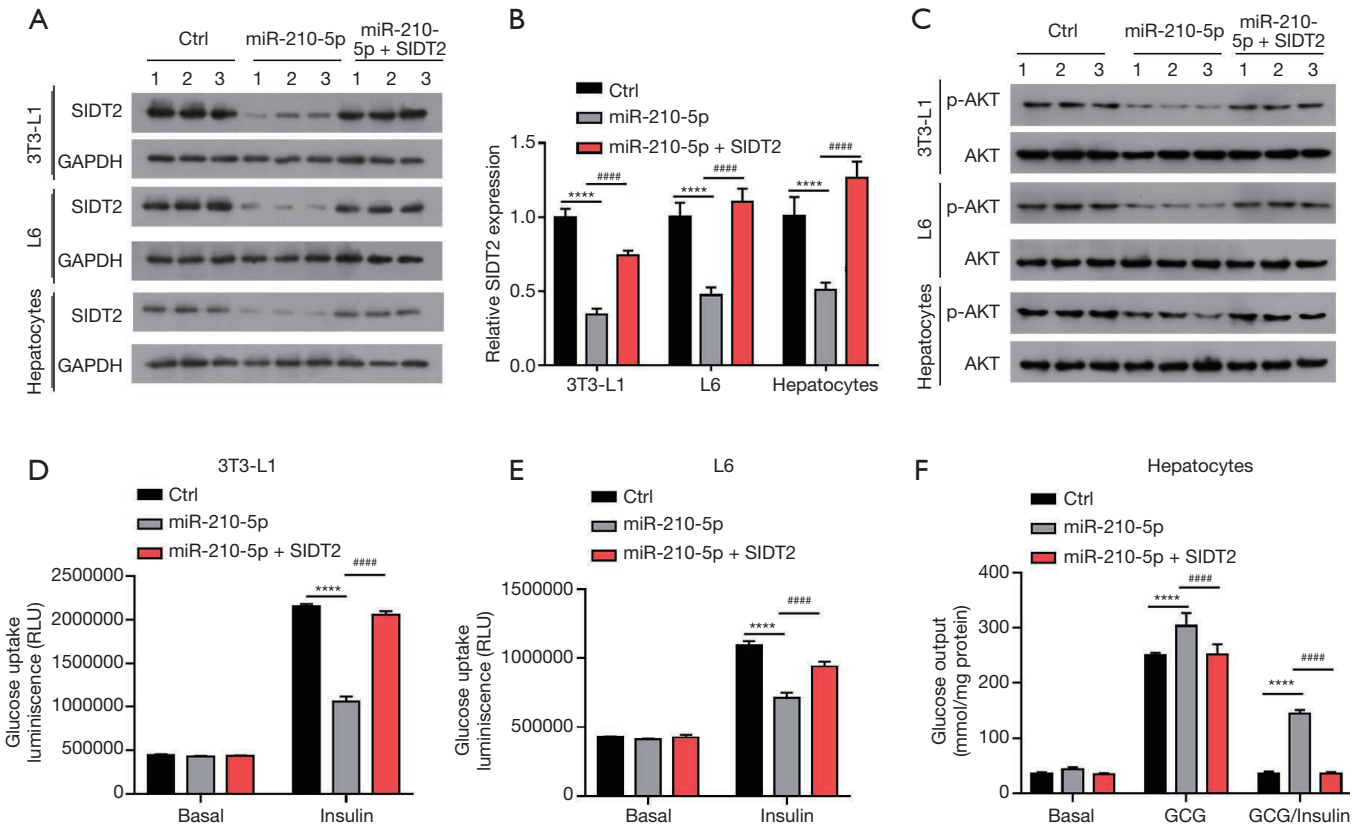

Figure 5 SIDT2 reversed the miR-210-5p–mediated effects on cellular insulin sensitivity. (A,B) The SIDT2 mRNA and protein expression in 3T3-L1 adipocytes, L6 myocytes, and primary hepatocytes cotransfected with miR-210-5p or control mimics and the SIDT2 plasmid. (C) Western blot analysis of p-AKT protein expression. (D-F) Glucose uptake capacity of 3T3-L1 adipocytes and L6 myocytes as well as the glucose production capacity of primary hepatocytes with the indicated treatments. Data are expressed as mean ± SD, n=3. ****, P<0.0001 *vs.* control group; ####, P<0.0001 *vs.* miR-210-5p group. GCG, glucagon; SIDT2, SID1 transmembrane family member 2; p-AKT, phosphorylated-protein kinase B.

inflammation, and insulin sensitivity (29-31). A recent study demonstrated that *SIDT2* knockout increased fasting blood glucose, impaired glucose tolerance *in vivo*, and reduced insulin-stimulated glucose uptake *in vitro* (32). Another study reported that SIDT2 promoted insulin secretion and lipid metabolism (28). In our study, the overexpression of SIDT2 reversed insulin-induced glucose uptake and glucose production suppression caused by the upregulation of miR-210-5p *in vitro*. Furthermore, the upregulation of SIDT2 inhibited the elevation of fasting blood glucose levels, fasting serum insulin, HOMA-IR, and glucose and insulin intolerance induced by the CUG-SGA-ATM-exos administration *in vivo*.

An essential mechanism of insulin resistance is the AKT signal pathway (33). Insulin resistance is mediated by the phosphorylation of AKT (34). It has been reported that both miR-210-5p and SIDT2 affect the AKT signal pathway (32,35). In line with is, our study found that miR-210-5p decreased the phosphorylation of AKT in 3T3-L1 adipocytes, L6 myocytes, and primary hepatocytes treated with insulin; however, this effect was reversed by the overexpression of SIDT2. Furthermore, SIDT2 treatment reversed the phosphorylation of AKT decrease caused by the administration of CUG-SGA-ATM-exos miR-210-5p.

Conclusions

Our study is the first to report that ATM–derived exosomal miR-210-5p can suppress the insulin sensitivity in CUG-SGA rats via the overexpression of SIDT2, suggesting that this miRNA may be used in a therapeutic approach for

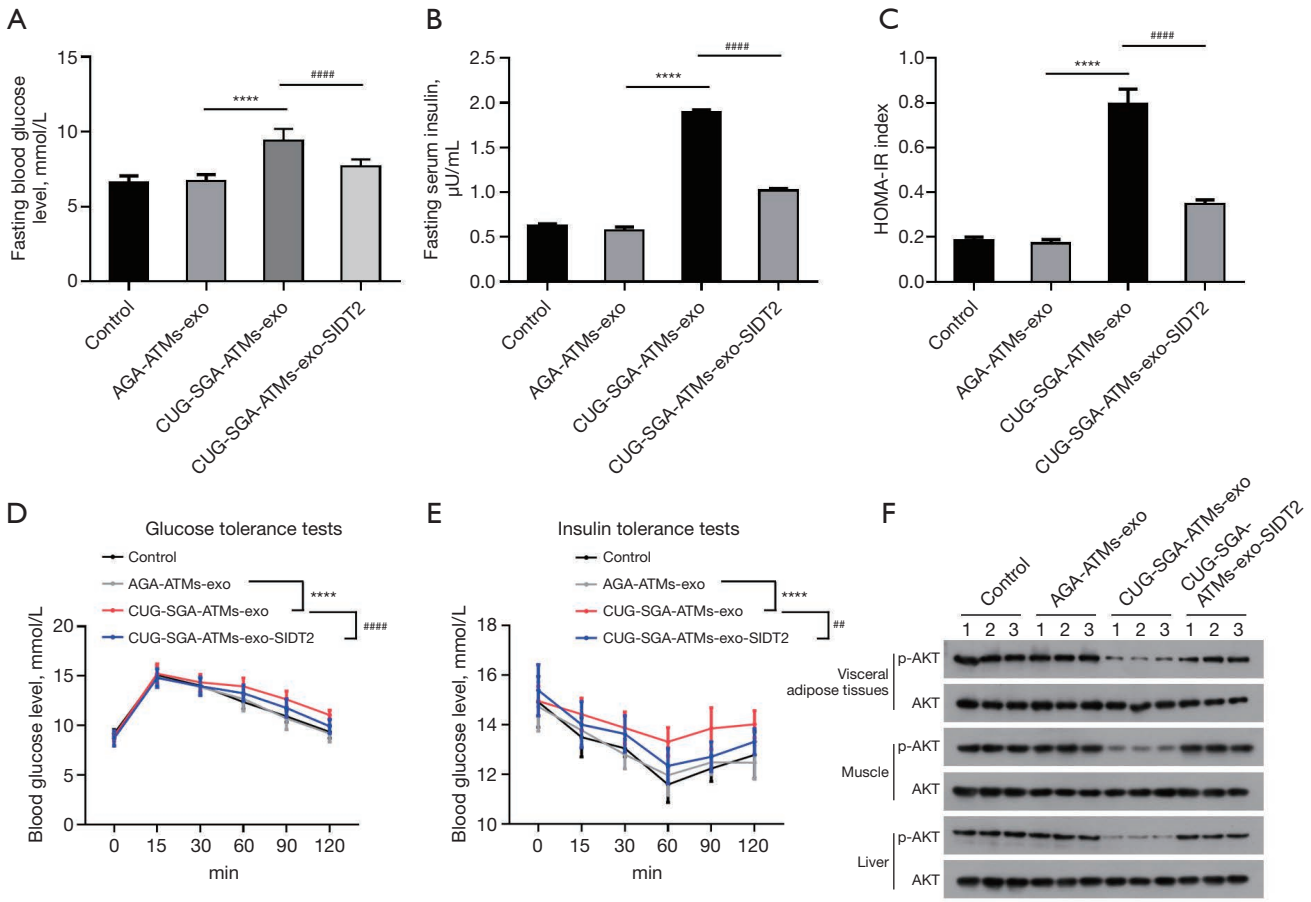

Figure 6 CUG-SGA ATMs-derived exosomal miR-210-5p enhanced insulin resistance *in vivo* via SIDT2. (A-E) The fasting blood glucose levels, fasting serum insulin, HOMA-IR, glucose tolerance, and insulin tolerance of AGA rats treated with CUG-SGA-ATMs-exo, AGA-ATMs-exo, or CUG-SGA-ATMs-exo and SIDT2 plasmid. (F) Phosphorylation of AKT in the liver, adipose, and muscle tissues from indicated rats. Data are expressed as mean ± SD, n=5. ****, P<0.0001 *vs.* AGA-ATMs-exo group; ##, P<0.01, ####, P<0.0001 *vs.* CUG-SGA-ATMs-exo group. HOMA-IR, homeostasis model assessment of the insulin resistance; AGA, adequate-for-gestational-age; CUG-SGA-ATMs, macrophages from adipose tissues of small-for-gestational-age with catch-up-growth; AKT, protein kinase B.

children born SGA with CUG.

Acknowledgments

Funding: None.

Footnote

Reporting Checklist: The authors have completed the ARRIVE reporting checklist. Available at https://tp.amegroups.com/article/view/10.21037/tp-23-142/rc

Data Sharing Statement: Available at https://tp.amegroups.com/article/view/10.21037/tp-23-142/dss

Peer Review File: Available at https://tp.amegroups.com/article/view/10.21037/tp-23-142/prf

Conflicts of Interest: All authors have completed the ICMJE uniform disclosure form (available at https://tp.amegroups.com/article/view/10.21037/tp-23-142/coif). The authors have no conflicts of interest to declare.

Ethical Statement: The authors are accountable for all aspects of the work in ensuring that questions related to the accuracy or integrity of any part of the work are appropriately investigated and resolved. All animal procedures complied with institutional guidelines for the care and use of animals, and the protocols were approved

by the Institutional Animal Ethics Committee of The Sixth Affiliated Hospital, Sun Yat-sen University (No. IACUC-2021092702).

References

1. Ko JM, Park HK, Yang S, et al. Influence of catch-up growth on IGFBP-2 levels and association between IGFBP-2 and cardiovascular risk factors in Korean children born SGA. Endocr J 2012;59:725-33.
2. Netchine I, van der Steen M, López-Bermejo A, et al. New Horizons in Short Children Born Small for Gestational Age. Front Pediatr 2021;9:655931.
3. Moon HS, Kim H, Kim B, et al. Mouse Model of Small for Gestational Age Offspring with Catch-up Growth Failure and Dysregulated Glucose Metabolism in Adulthood. J Obes Metab Syndr 2022;31:81-5.
4. Campisi SC, Carbone SE, Zlotkin S. Catch-Up Growth in Full-Term Small for Gestational Age Infants: A Systematic Review. Adv Nutr 2019;10:104-11.
5. Ruys CA, Hollanders JJ, Bröring T, et al. Early-life growth of preterm infants and its impact on neurodevelopment. Pediatr Res 2019;85:283-92.
6. Osborn O, Olefsky JM. The cellular and signaling networks linking the immune system and metabolism in disease. Nat Med 2012;18:363-74.
7. Olefsky JM, Glass CK. Macrophages, inflammation, and insulin resistance. Annu Rev Physiol 2010;72:219-46.
8. Liu C, Wu B, Lin N, et al. Insulin resistance and its association with catch-up growth in Chinese children born small for gestational age. Obesity (Silver Spring) 2017;25:172-7.
9. Deng HZ, Deng H, Su Z, et al. Insulin resistance and adiponectin levels are associated with height catch-up growth in pre-pubertal Chinese individuals born small for gestational age. Nutr Metab (Lond) 2012;9:107.
10. Cho WK, Suh BK. Catch-up growth and catch-up fat in children born small for gestational age. Korean J Pediatr 2016;59:1-7.
11. Lian QX, Deng HZ, Chen KY, et al. Role of Peroxisome Proliferator-Activated Receptor (PPARgamma) in Metabolic Disorders in SGA with Catch-Up Growth. Obesity (Silver Spring) 2018;26:88-93.
12. Tian F, Tang P, Sun Z, et al. miR-210 in Exosomes Derived from Macrophages under High Glucose Promotes Mouse Diabetic Obesity Pathogenesis by Suppressing NDUFA4 Expression. J Diabetes Res 2020;2020:6894684.
13. Li L, Zuo H, Huang X, et al. Bone marrow macrophage-derived exosomal miR-143-5p contributes to insulin resistance in hepatocytes by repressing MKP5. Cell Prolif 2021;54:e13140.
14. Ji Y, Luo Z, Gao H, et al. Hepatocyte-derived exosomes from early onset obese mice promote insulin sensitivity through miR-3075. Nat Metab 2021;3:1163-74.
15. Kumar A, Ren Y, Sundaram K, et al. miR-375 prevents high-fat diet-induced insulin resistance and obesity by targeting the aryl hydrocarbon receptor and bacterial tryptophanase (tnaA) gene. Theranostics 2021;11:4061-77.
16. Wei L, Zhao D. M2 macrophage-derived exosomal miR-145-5p protects against the hypoxia/reoxygenation-induced pyroptosis of cardiomyocytes by inhibiting TLR4 expression. Ann Transl Med 2022;10:1376.
17. Ying W, Riopel M, Bandyopadhyay G, et al. Adipose Tissue Macrophage-Derived Exosomal miRNAs Can Modulate In Vivo and In Vitro Insulin Sensitivity. Cell 2017;171:372-384.e12.
18. Dang SY, Leng Y, Wang ZX, et al. Exosomal transfer of obesity adipose tissue for decreased miR-141-3p mediate insulin resistance of hepatocytes. Int J Biol Sci 2019;15:351-68.
19. Maixner N, Haim Y, Blüher M, et al. Visceral Adipose Tissue E2F1-miRNA206/210 Pathway Associates with Type 2 Diabetes in Humans with Extreme Obesity. Cells 2022;11:3046.
20. Deng HZ, Deng H, Li YH, et al. Effects of a high-protein diet on insulin resistance and body fat in catch-up growth rats born small for gestational age. Horm Res Paediatr 2012;78:180-7.
21. An J, Wang J, Guo L, et al. The Impact of Gut Microbiome on Metabolic Disorders During Catch-Up Growth in Small-for-Gestational-Age. Front Endocrinol (Lausanne) 2021;12:630526.
22. García JG, Ansorena E, Milagro FI, et al. Endothelial Nox5 Expression Modulates Glucose Uptake and Lipid Accumulation in Mice Fed a High-Fat Diet and 3T3-L1 Adipocytes Treated with Glucose and Palmitic Acid. Int J

Mol Sci 2021;22:2729.
23. Hou WL, Yin J, Alimujiang M, et al. Inhibition of mitochondrial complex I improves glucose metabolism independently of AMPK activation. J Cell Mol Med 2018;22:1316-28.
24. Zhu J, Liu B, Wang Z, et al. Exosomes from nicotine-stimulated macrophages accelerate atherosclerosis through miR-21-3p/PTEN-mediated VSMC migration and proliferation. Theranostics 2019;9:6901-19.
25. Long R, Gao L, Li Y, et al. M2 macrophage-derived exosomes carry miR-1271-5p to alleviate cardiac injury in acute myocardial infarction through down-regulating SOX6. Mol Immunol 2021;136:26-35.
26. Ying W, Gao H, Dos Reis FCG, et al. MiR-690, an exosomal-derived miRNA from M2-polarized macrophages, improves insulin sensitivity in obese mice. Cell Metab 2021;33:781-790.e5.
27. Nguyen TA, Bieging-Rolett KT, Putoczki TL, et al. SIDT2 RNA Transporter Promotes Lung and Gastrointestinal Tumor Development. iScience 2019;20:14-24.
28. Moon S, Lee Y, Won S, et al. Multiple genotype-phenotype association study reveals intronic variant pair on SIDT2 associated with metabolic syndrome in a Korean population. Hum Genomics 2018;12:48.
29. Geng MY, Wang L, Song YY, et al. Sidt2 is a key protein in the autophagy-lysosomal degradation pathway and is essential for the maintenance of kidney structure and filtration function. Cell Death Dis 2021;13:7.
30. Chen X, Gu X, Zhang H. Sidt2 regulates hepatocellular lipid metabolism through autophagy. J Lipid Res 2018;59:404-15.
31. Sun H, Ding JM, Zheng HH, et al. The Effects of Sidt2 on the Inflammatory Pathway in Mouse Mesangial Cells. Mediators Inflamm 2020;2020:3560793.
32. Xiong QY, Xiong CQ, Wang LZ, et al. Effect of sidt2 Gene on Cell Insulin Resistance and Its Molecular Mechanism. J Diabetes Res 2020;2020:4217607.
33. Chen SH, Liu XN, Peng Y. MicroRNA-351 eases insulin resistance and liver gluconeogenesis via the PI3K/AKT pathway by inhibiting FLOT2 in mice of gestational diabetes mellitus. J Cell Mol Med 2019;23:5895-906.
34. Zhang Z, Liu H, Liu J. Akt activation: A potential strategy to ameliorate insulin resistance. Diabetes Res Clin Pract 2019;156:107092.
35. Liu W, Jiang D, Gong F, et al. miR-210-5p promotes epithelial-mesenchymal transition by inhibiting PIK3R5 thereby activating oncogenic autophagy in osteosarcoma cells. Cell Death Dis 2020;11:93.

Cite this article as: Xiong H, Liu W, Song J, Gu X, Luo S, Lu Z, Hao H, Xiao X. Adipose tissue macrophage-derived exosomal miR-210-5p in modulating insulin sensitivity in rats born small for gestational age with catch-up growth. Transl Pediatr 2023;12(4):587-599. doi: 10.21037/tp-23-142

Supplementary

Table S1 The sequences of all indicated primers used in this study

Gene	Sequences
rno-miR-210-5p-RT	5’ GTCGTATCCAGTGCAGGGTCCGAGGTATTCGCACTGGATACGACCAGTGT 3’
rno-miR-210-5p-F	5’ GTTAAGCCACTGCCCACAGC 3’
Universe-R	5’ GTGCAGGGTCCGAGGT 3’
rno-U6-F	5’ CTCGCTTCGGCAGCACA 3’
rno-U6-R	5’ AACGCTTCACGAATTTGCGT 3’
mmu-U6-F	5’ CTCGCTTCGGCAGCACATATACT 3’
mmu-U6-R	5’ ACGCTTCACGAATTTGCGTGTC 3’
mmu-miR-210-5p-RT	5’ GTCGTATCCAGTGCAGGGTCCGAGGTATTCGCACTGGATACGACCAGTGT 3’
mmu-miR-210-5p-F	5’ GTTAAGCCACTGCCCACCGC 3’
Universe-R	5’ GTGCAGGGTCCGAGGT 3’
mmu-β-actin-F	5’ TCAGGGAGTAATGGTTGGAAT 3’
mmu-β-actin-R	5’ GGTCTCAAACATAATCTGGGTCA 3’
mmu-SIDT2-F	5’ CAACGCCAGTGCCTACAGTG 3’
mmu-SIDT2-R	5’ GAGCAGGGTGGAGATGATGT 3’
rno-β-actin-F	5’ AGGCCAACCGTGAAAAGATG 3’
rno-β-actin-R	5’ ATGCCAGTGGTACGACCAGA 3’
rno-SIDT2-F	5’ CACCTCATCCTACCAGCCACTA 3’
rno-SIDT2-R	5’ CCTCTGGACATTCTTGGGCA 3’

https://dx.doi.org/10.21037/tp-23-142